AD-A077 060 ROCKWELL INTERNATIONAL ANAHEIM CA AUTONETICS STRATEG--ETC F/G 9/3
FLAT BUS FAULT SENSORS.(U)
OCT 79 C O LINDER
UNCLASSIFIED C79-951-201 NADC-77336-60 N62269-78-C-0213 NL

1 OF 1
AD-
A077060

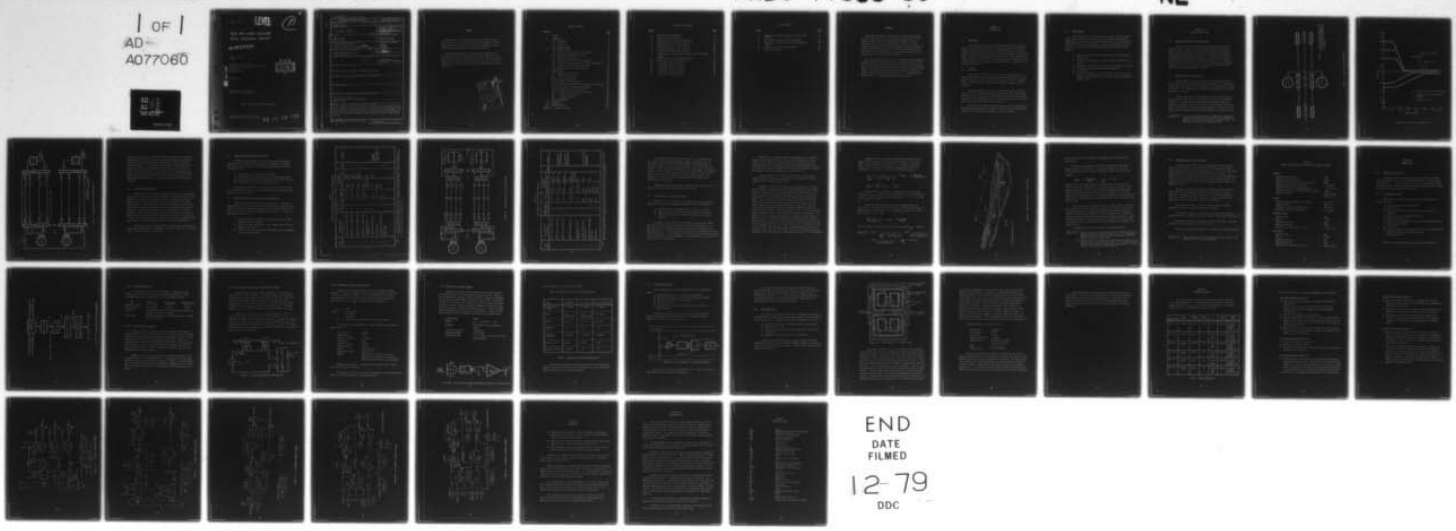

END
DATE
FILMED
12-79
DDC

NADC 77336-60

LEVEL II

FLAT BUS FAULT SENSORS
FINAL TECHNICAL REPORT

AD A077060

CARL O. LINDER
Author

ROCKWELL INTERNATIONAL
AUTONETICS STRATEGIC SYSTEMS DIVISION
3370 MIRALOMA AVENUE
P.O. BOX 4193
ANAHEIM, CA 92803

OCTOBER 1979

FINAL REPORT, FIRST DRAFT
OCTOBER 1978 TO OCTOBER 1979

NAVAL AIR DEVELOPMENT CENTER
WARMINSTER, PENNSYLVANIA 18974

UNCLASSIFIED

SECURITY CLASSIFICATION OF THIS PAGE (When Data Entered)

REPORT DOCUMENTATION PAGE	READ INSTRUCTIONS BEFORE COMPLETING FORM
1. REPORT NUMBER: NADC 77336-60	2. GOVT ACCESSION NO. / 3. RECIPIENT'S CATALOG NUMBER
4. TITLE (and Subtitle): FLAT BUS FAULT SENSORS	5. TYPE OF REPORT & PERIOD COVERED: TECHNICAL - FINAL rept. OCT 1978 — OCT 1979
	6. PERFORMING ORG. REPORT NUMBER: C79-951-201
7. AUTHOR(s): Carl O. LINDER	8. CONTRACT OR GRANT NUMBER(s): N62269-78-C-0213
9. PERFORMING ORGANIZATION NAME AND ADDRESS: ROCKWELL INTERNATIONAL, AUTONETICS STRATEGIC SYSTEMS DIVISION, 3370 MIRALOMA AVE., P.O. BOX 4192, ANAHEIM, CA 92803	10. PROGRAM ELEMENT, PROJECT, TASK AREA & WORK UNIT NUMBERS: AIRTASK WFI-400000
11. CONTROLLING OFFICE NAME AND ADDRESS: NAVAL AIR DEVELOPMENT CENTER, WARMINSTER, PA 18974	12. REPORT DATE: OCT 1979 / 13. NUMBER OF PAGES: 48
14. MONITORING AGENCY NAME & ADDRESS (if different from Controlling Office)	15. SECURITY CLASS. (of this report): UNCLASSIFIED / 15a. DECLASSIFICATION/DOWNGRADING SCHEDULE

16. DISTRIBUTION STATEMENT (of this Report)

APPROVED FOR PUBLIC RELEASE; DISTRIBUTION UNLIMITED

17. DISTRIBUTION STATEMENT (of the abstract entered in Block 20, if different from Report)

18. SUPPLEMENTARY NOTES

19. KEY WORDS (Continue on reverse side if necessary and identify by block number)

FLAT BUS FAULT SENSORS
POWER DISTRIBUTION FAULT SENSOR SYSTEM
CURRENT SENSOR

20. ABSTRACT (Continue on reverse side if necessary and identify by block number)

This report documents the development of an electric power distribution fault sensing technique for use on a 270 Vdc, two wire, flat bus, ungrounded aircraft power distribution system for operation in composite aircraft structures. The effort, performed by the Strategic Systems Division of Rockwell International, included the development, fabrication and delivery of six fault sensor breadboards.

DD FORM 1 JAN 73 1473 EDITION OF 1 NOV 65 IS OBSOLETE

UNCLASSIFIED 391 827

SECURITY CLASSIFICATION OF THIS PAGE (When Data Entered)

PREFACE

This document is the final technical report for the Flat Bus Fault Sensor Study. The work was performed by Autonetics Strategic Systems Division of Rockwell International Corporation, Anaheim, California under NADC Contract Number N62269-78-C-0213.

The major contributions to sensor development were made by G. L. Schmitt of the Stragetic Systems Division of Rockwell International; the preliminary power distribution and sensor system and the 270 volt dc generator performance criteria were derived from work performed by J. Frencho of the Columbus Division of Rockwell International.

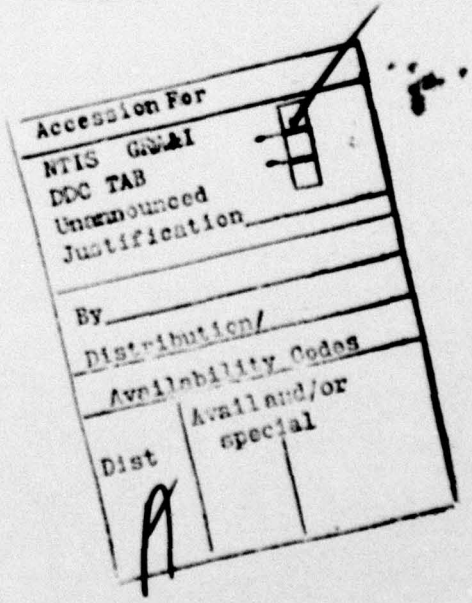

TABLE OF CONTENTS

LIST OF ILLUSTRATIONS

LIST OF TABLES

SUMMARY

This report documents the Flat Bus Fault Sensor Study performed by the Strategic Systems Division of Rockwell International. The purpose of the study was to investigate and develop an electric power distribution fault sensing technique for use on a 270 Vdc, two-wire, ungrounded aircraft power distribution system for operation in composite aircraft structures. The effort included the development, fabrication and delivery of six fault sensor breadboards suitable for use in a laboratory system simulator.

The study developed a fault sensor system based on power generation performance criteria described in the design specification for a 270 volt direct current aircraft generator system prepared by the Columbus Division of Rockwell International for the Naval Air Development Center (NADC). The sensor system required the development of overcurrent, undervoltage and differential current sensors. Six breadboards with various designs of these sensors were delivered to NADC.

SECTION II
INTRODUCTION

2.1 Background

The introduction of aircraft structures fabricated with composite materials may eliminate the option of using the aircraft structure as an electrical power system return path. An ungrounded two-wire power distribution system has been considered to fulfill the new operational requirements. Studies have shown that flat conductor power feeders can provide a greater surface for heat transfer than round conductors. Therefore, a flat conductor power bus in a sandwich type construction is anticipated for use in the two-wire system.

2.2 Objective

The objective of the Flat Bus Fault Sensor Study (FBFS) was to investigate and develop electrical power distribution fault sensing techniques and sensors for use in a 270 volt dc, two-wire flat bus, ungrounded aircraft power distribution system for operation in composite aircraft structures.

The system operational goal was a coordinated system of sensors which could provide distribution zone protection and fault isolation and interface with the Advanced Aircraft Electrical System (AAES) load management system. The development goal was to develop fault sensors that would sense line-to-line and line-to-structure faults.

The study also required the delivery of six sensor breadboards to the Naval Air Development Center (NADC) that could be used to demonstrate the feasibility of the sensing concept in a system simulator.

2.3 Study Approach

Prior to the award of the Flat Bus Sensor Study contract, Rockwell International developed a preliminary power distribution fault sensing system based on known NADC requirements and on a power system derived from prior V/STOL aircraft and AAES studies. Rockwell International's approach to achieve the FBFS design objectives therefore followed the following sequence:

1) Review of the aircraft electric power system derived from the prior studies.
2) Description and analysis of a fault sensing system based on 1) above.
3) Optimization of the fault sensing system described in 2) above.
4) Development of general sensor design requirements.
5) Sensor design.
6) Fabrication, assembly, test and delivery of the sensor breadboards to NADC, together with this final report and breadboard design drawings.

SECTION III
FAULT SENSING SYSTEM

3.1 Typical Aircraft Electric Power System

A typical aircraft electrical power generation and distribution system is shown in Figure 1. It is based on Rockwell International's Type "A" V/STOL aircraft configuration and depicts the total continuous load distribution throughout the aircraft. Power from the generators is transmitted into the Central Electronics Distribution Center and then to remote distribution centers throughout the aircraft via bus feeders. The bus voltage characteristics (see Figure 2) were developed by Rockwell International as part of a design specification for a 270 Vdc aircraft generating system (see Reference (a) below).

3.2 Preliminary Fault Sensor System

The bus feeder from the Central Electronic Distribution Center to the AFT Electronic Distribution Center was selected in the prior study as the power distribution zone to be protected by a sensor system as shown in Figure 3. This sensor system will hereafter be referred to as the preliminary sensor system.

The bus feeder consisted of redundant positive and negative flat bus conductors to provide full rated capability upon loss of one feeder conductor. As shown, the selected bus feeder would have a continous rating of 100 amperes, 270 Vdc to allow for 25% system growth. Since the design characteristics of a sensor are independent of the subordinate bus function, the subordinate busses (essential, monitor, secondary, etc.) are

---

Reference (a): Rockwell International Report No. NR75H-158, "Development of a Design Specification for 270 Volt Direct Current, Oil Cooled, Aircraft Generating System", dated March 1976, Crow and Frencho, NADC Contract N62269-75-C-0399.

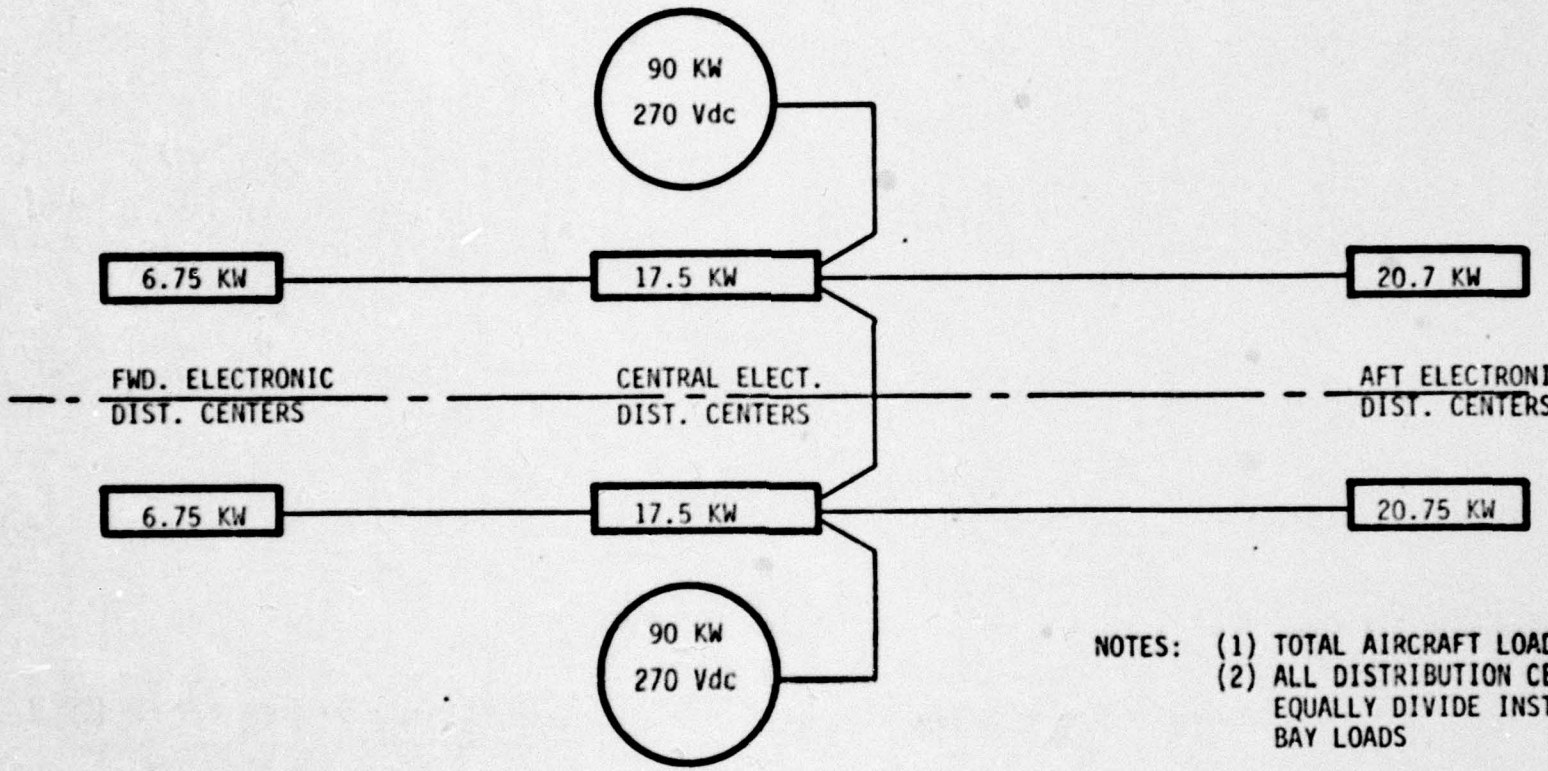

NOTES: (1) TOTAL AIRCRAFT LOAD : 90 KW
(2) ALL DISTRIBUTION CENTERS EQUALLY DIVIDE INSTALLATION BAY LOADS

FIGURE (1). ELECTRIC LOAD DISTRIBUTION

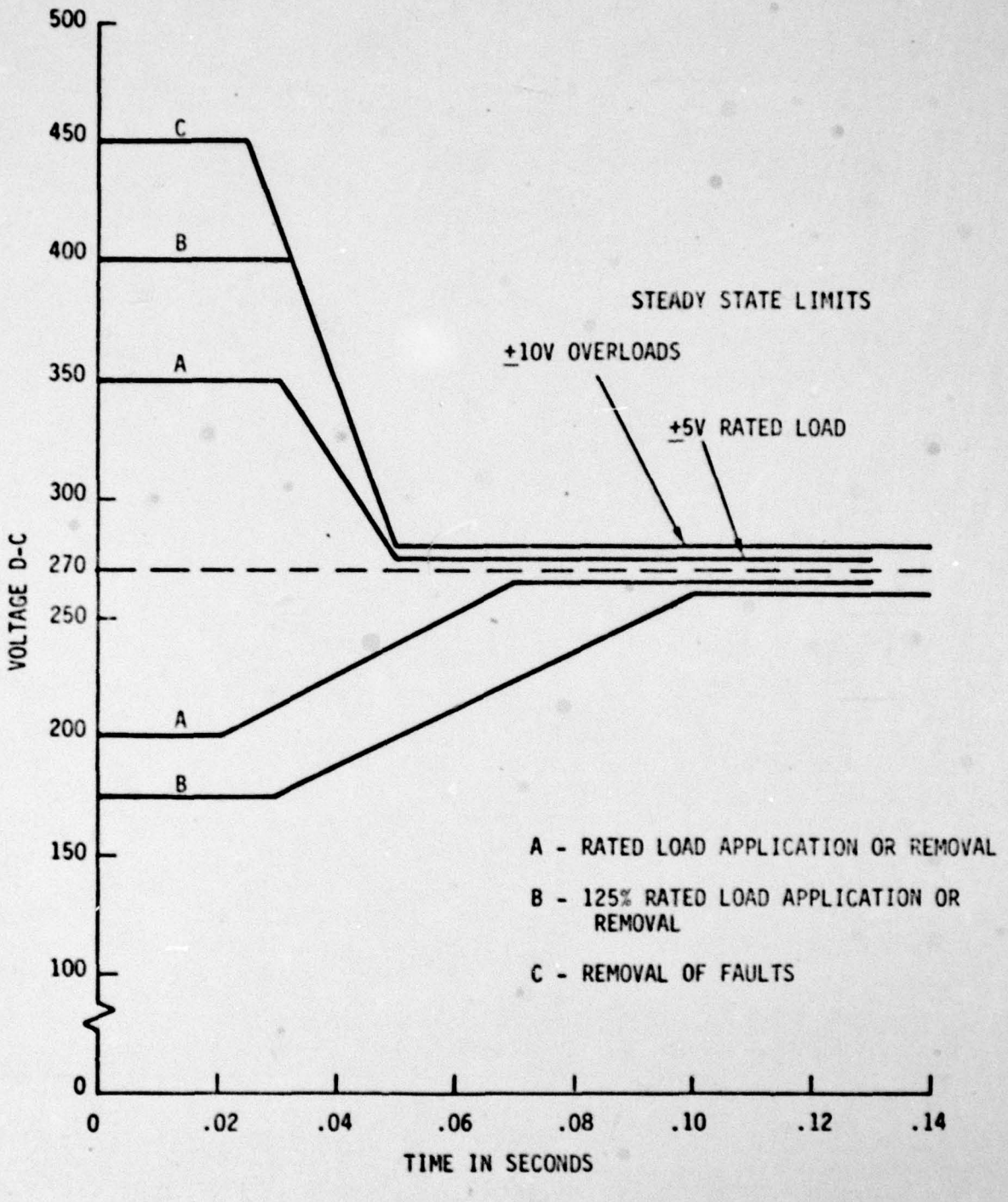

FIGURE (2). BUS VOLTAGE CHARACTERISTICS

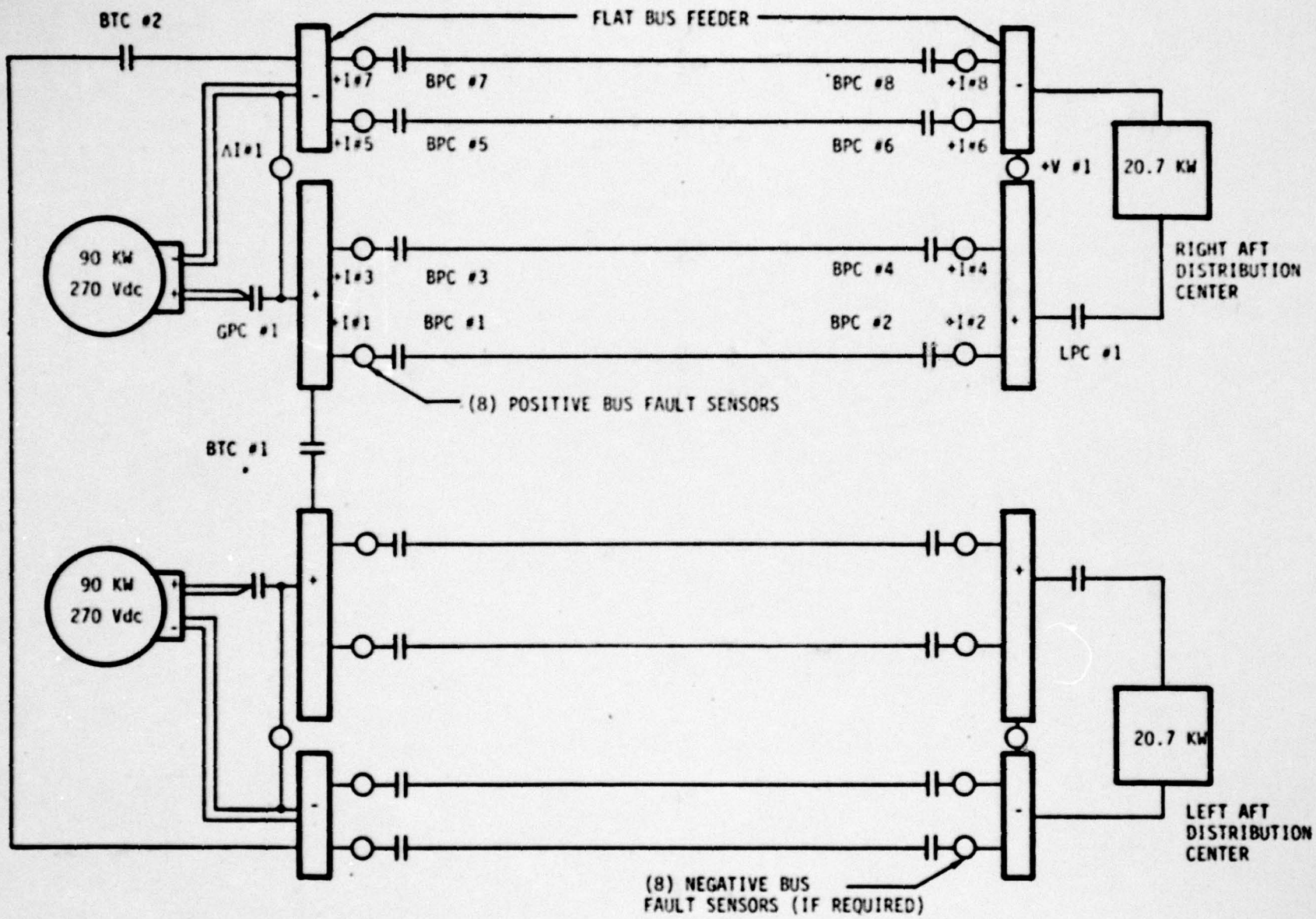

FIGURE (3). PRELIMINARY SENSOR SYSTEM CONFIGURATION

not depicted in Figure 3. The fault sensing system had sensors installed at each end of the flat bus feeder, thereby providing full zone protection from the Central Electronics Distribution Center to the AFT Electronics Distribution Center. Total isolation of the feeder segment necessitated power interruptors, e.g. Bus Power Controllers (BPC), to be installed within this zone of protection. The function of the fault sensor was to detect a fault within its zone of protection and cause the faulted segment to be totally disconnected from the power generation system and its load before the protection functions of the power generation system reacted to the fault.

3.3 Bus Fault Characteristics

The bus faults that will be encountered in the Figure 3 configuration include (1) Single Positive-to-Negative Feeder, (2) Double Positive-to-Single Negative, (3) Single Positive-to-Double Negative, (4) Double Positive-to-Double Negative, (5) Positive-to-Structure and (6) Negative-to-Structure. The first four (4) fault types are classic, with resultant excessive current and decreased voltage, the magnitude of each being dependent upon the fault impedance. These faults are detected by the overcurrent (+I) and undervoltage (+V) sensors (refer to Figure 3). Faults (5) and (6) are defined as ground faults and are detected by a differential (ΔI) sensor. The operation of the ΔI Sensor is dependent upon the aircraft structure and grounding technique employed. The need for such a sensor is discussed in Paragraph 3.6.

The operation of the right aft feeder bus fault sensors (see Figure 3) is described in Paragraph 3.4. An analysis of the left aft system is not shown since it would be identical to the former.

3.4 Analysis of Preliminary Sensor System

Analysis of the operation of the preliminary sensor system when subjected to the fault conditions described in Paragraph 3.3, provides the results listed in Table 1. The following conditions can be derived from these results:

1) +I sensors 2, 4, 6 and 8 are not required.
2) Fault numbers 4, 5, 9 and 10 require a backup power source.
3) A "200 ampere" fault in fault condition #4 would be undetected.
4) BTC #2 does not perform any useful function.

It would be desirable to re-configure the system to derive maximum use of the existing generators and eliminate the need for the backup power source indicated in 2) above.

3.5 Proposed Flat Bus Fault Sensor System Configuration

Consider the distribution system shown in Figure 4. Performing a fault analysis on the latter configuration (see Table 2) indicates that the Figure 4 configuration reduces the number of sensors required from 20 to 14 and only increases the number of controllers from 21 to 23. It also adds the following capability:

1) BTC #2 eliminates the need for backup power source for fault conditions 4 and 9, Table 1.
2) BTC #3 eliminates the need for a backup power source for fault condition #10, Table 1.
3) Sensor +I #9 will indicate the "200 ampere fault" in Paragraph 3.4, conclusion 3) above.

TABLE 1.

RESPONSE OF PRELIMINARY SENSOR SYSTEM TO A FAULT CONDITION

FAULT CONDITION	BUS DISTRIBUTION FEEDER FAULT	FAULT TYPE		SENSOR ACTIVATED	ANTICIPATED PC ACTION		NOTE	REMARKS
		SHORT	OPEN		IMMEDIATE	FINAL		
1	SINGLE PLUS TO SINGLE MINUS	X		+I #3, #5	OPEN BPC 3 - 6	LEAVE BPC 5 - 6 OPEN	1	
2	DOUBLE PLUS TO SINGLE MINUS	X		+I #1, #3, #5	OPEN BPC 1 - 6	LEAVE BPC 5 - 6 OPEN	1	
3	SINGLE PLUS TO DOUBLE MINUS	X		+I #3, #5, #7	OPEN BPC 3 - 8	LEAVE BPC 3, 4 OPEN	1	
4	DOUBLE PLUS TO DOUBLE MINUS	X		+I #1, #3, #5, #7	OPEN BPC 1 - 8		1, 2	
5	SINGLE OR DOUBLE PLUS TO STRUCTURE	X		ΔI #1	OPEN GPC 1, BPC 1 - 4	SAME		
6	STRUCTURE TO SINGLE MINUS	X		NONE	NONE	NONE		NO ACTION REQUIRED
7	EXCESSIVE LOAD			+I #1 - #8	OPEN LPC 1			LOCAL LOAD PC's SHOULD TRIP
8	SINGLE PLUS OR SINGLE MINUS		X	NONE	NONE			
9	DOUBLE PLUS		X	+V #1			2	
10	DOUBLE MINUS		X	+V #1			2	

NOTE: (1) The "final" PC action assumes that either a positive or a negative feeder line fault can continue in operation after a fault between the two is detected by removal from operation of either side of the fault.

(2) Requires switching to a backup power source.

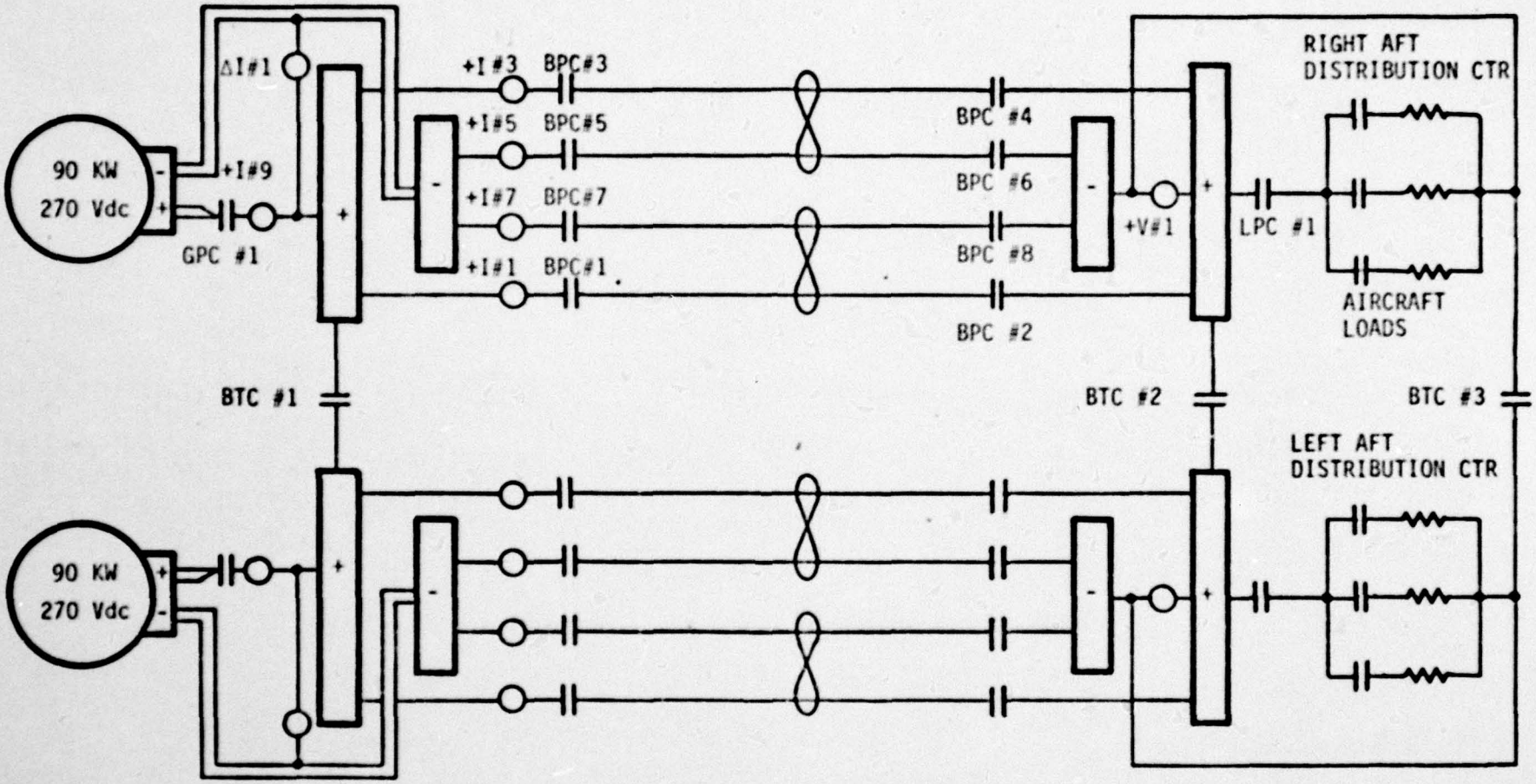

FIGURE (4). PROPOSED SENSOR SYSTEM CONFIGURATION

TABLE 2.

FBFS SYSTEM RESPONSE TO A FAULT CONDITION

FAULT NUMBER	BUS DISTRIBUTION FEEDER FAULT	FAULT TYPE		SENSOR ACTIVATED	ANTICIPATED PC ACTION		NOTE	REMARKS
		SHORT	OPEN		IMMEDIATE	FINAL		
1	SINGLE PLUS TO SINGLE MINUS	X		+I #3, #5	OPEN BPC #3 - #6	LEAVE BPC #5 - #6 OPEN	1	
2	DOUBLE PLUS TO SINGLE MINUS	X		+I #1, #3, #5	OPEN BPC #1 - #6	LEAVE BPC #5 - #6	1	This fault not likely, due to separated cables.
3	SINGLE PLUS TO DOUBLE MINUS	X		+I #3, #5, #7	OPEN BPC #3 - #8	LEAVE BPC #3, #4 OPEN	1	This fault not likely, due to separated cables.
4	DOUBLE PLUS TO DOUBLE MINUS	X		+I #1, #3, #5, #7	OPEN BPC #1 - #8	LEAVE BPC #1 - #4 OPEN, CLOSE BPC #1, #2	1	
5	SINGLE OR DOUBLE PLUS TO STRUCTURE	X		ΔI #1	OPEN GPC 1 BPC 1 - 4	SAME		
6	STRUCTURE TO SINGLE MINUS	X		NONE	NONE	NONE		No Action required
7	EXCESSIVE LOAD			+I #1 - #8	OPEN LPC 1			Local load PC's should trip.
8	SINGLE PLUS OR SINGLE MINUS		X	NONE	NONE	NONE		
9	DOUBLE PLUS		X	+V #1	CLOSE BTC 1, 2			
10	DOUBLE MINUS		X	+V #1	CLOSE BTC 1, 3			

NOTE: The "final" PC actfon assumes that either a positive or a negative feeder line fault can continue in operation after a fault between the two is detected by removal from operation of either side of the fault.

To provide additional fail-safe margins, it is recommended that the number of flat bus cables laminated together be two (one "plus" and one "minus" return), rather than the four cables laminated together as implied in Figure 3. An undetected high current fault in one of the four cables is likely to damage all four cables due to overheating. Also, battle damage is much more likely to short or open four cables laminated together than two sets of two cables separated by some moderate distance. The difference in immunity to EMP and the generation of additional EMI is considered to be negligible.

The power distribution and sensor system shown in Figure 4 is proposed as the fault detection system for the FBFS study.

3.6 Ground Faults In Composite Structure

Detection of ground faults in an aircraft fabricated with composite materials and employing an ungrounded power system has to be preceded by:

1) Definitions of an ungrounded power system in an aircraft.
2) Description of the characteristics of composite structures.
3) Grounding requirements in aircraft fabricated with composite material.

An ungrounded power system in an aircraft, as defined here, refers to a power system electrically isolated from the aircraft structure. It is electrically isolated because the aircraft structure is considered to be non-conductive, i.e., fabricated with a composite of fiber laminates relatively high in resistance. It it is assumed for the moment that the aircraft structure is made up entirely of composite materials, the contributions of the latter to ground faults can be evaluated.

Currently, the composite material most commonly used for aircraft structures is composed of graphite fibers laminated together with epoxy resin. The end product has a low resistance (approximately 10Ω/sq. ft.) along the fibers and a relatively high resistance (approximately 20KΩ/sq. ft.) from side to side or through the resin and across the fibers. Segments of composite structures are separated by a resistance $>10^{12}\Omega$.

A single fault to the distribution bus within a segment of the composite structure requires a return path to cause current to flow and therefore, will not cause a fault current.

A double fault within the segment will cause currents in a fault sensor. However, it would require sensing the differential current between a sensor in the fault area and a sensor outside of the fault area. Practically speaking, this would mean continuous comparison of the absolute magnitude of all bus current sensors located between the source and the loads. A lower reading by one or more sensors, of course, implies that the difference current is being by-passed around the sensor(s). Such a sensing capability, sensing absolute magnitude changes on the order of 6 mA - not 6 mA differences between two current, requires each sensor to output and SOSTEL (SOSTEL - SOlid State Electric Logic - is a Naval aircraft power management system) to read the current magnitude of each sensor. This would constitute a significant complication to sensor and SOSTEL designs. The probability of a double fault between the insulated positive portion of the distribution bus and the insulated composite structure (each fault would have to penetrate the resin) is very low and the cost of increasing the capability of SOSTEL would probably be high. The damage caused by this type of fault would most likely be a local deterioration of the laminated structure. Therefore, adding the capability to sense this type of fault is not recommended.

A double fault to two isolated segments of the structure would produce fault currents that are virtually undetectable. A worst case fault is shown in Figure 5, where Fault No. 1 is shorted to Composite Structure No. 1, Fault No. 2 is shorted to Composite Structure No. 2 and Structures 1 and 2 are insulated to avoid galvanic reactions.

$$\frac{1}{\frac{1}{R_{LINE}} + \frac{1}{R_{S1} + R_{S2} + RI}} \times I_{LINE} = E_L \text{ (LINE DROP BETWEEN FAULTS)}$$

$$\frac{E_L}{R_{S1} + R_{S2} + R_I} = I_{FAULT}$$

Assume Fault No. 1 punctures the graphite fiber and the sheet resistance is $R_{S1} = 10\Omega/\square$. Also assume Fault No. 1 is 1 foot from the insulation space and the structure is 1 foot wide; $\therefore$ 1' X 1' = 1 $\square$' and $R_{S1} = 10\Omega/\square \times 1\square = 10\Omega$.

Assume Fault No. 2 does not puncture the graphite fiber and $R_{S2} = 20K\Omega/\square$. Also assume Fault is 1 foot from the insulation space and the structure is 1 foot wide; 1'X 1' = 1$\square$ and $R_{S2} = 20K\Omega\square \times 1\square = 20K\Omega$. Also assume $R_I \simeq 10^{12}\Omega$. Then

$$\frac{E_{LINE\ DROP}}{10\Omega + 20K\Omega + 10^{12}} = I_{FAULT} = \frac{E_{LINE\ DROP}}{10^{12}}$$

The line resistance is small but assume 0.1Ω and assume $I_{LINE} = 400$ amps.

$$E_{LINE\ DROP} = I_{LINE} \times \frac{1}{\frac{1}{R_{LINE}} + \frac{1}{R_{S1} + R_{S2} + R_I}} = 400 \frac{1}{\frac{1}{0.1\Omega} + \frac{1}{10\Omega + 20K\Omega + 10^{12}\Omega}}$$

$$= 400 \frac{1}{10 + 00.00008 \times 10^{-15}} = \frac{400}{10} = 40 \text{ volts}$$

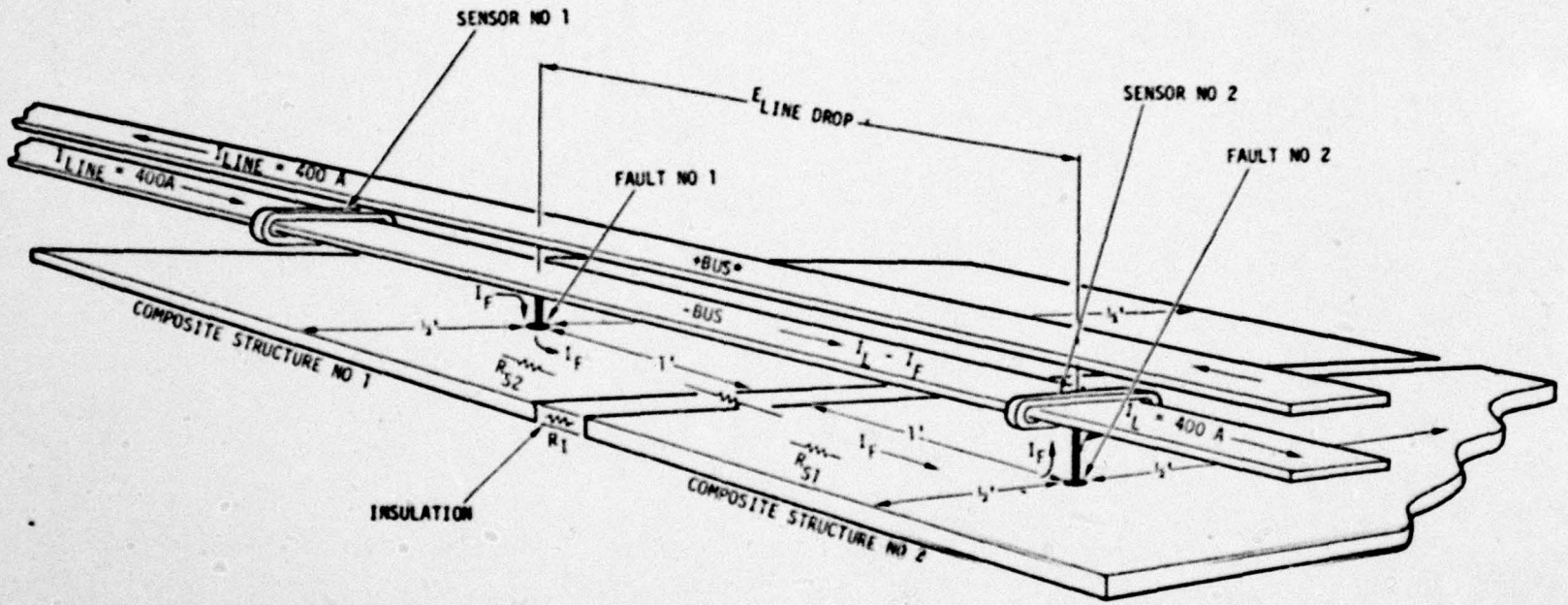

++Bus Sensors Omitted for Clarity

Figure 5. Double Ground Fault - Two Structures

As you would expect, the line drop is controlled by line resistance and line current.

Using these assumptions, we arrive at a 40 volt line drop in the feeder bus across the fault area - a ridiculous assumption - but using the 40 volt drop derived from these assumptions, look at the fault current (I_{FAULT}):

$$I_{FAULT} = \frac{E_{LINE\ DROP}}{10^{12}} = \frac{40}{10^{12}} = 40\ pA$$

Even with this ridiculously large line drop, we have a low level current that is practically undetectable in a circuit that has a normal full scale range of 400 amperes. From this, it is apparent that current differences, while adequate for many fault conditions, will not detect the small fault currents of a double ground fault to a composite structure using an ungrounded power system. The detection of a single ground fault in such a system is even more difficult.

Thus, the detection of ground faults in a purely composite structure does not seem to be either necessary or economical. However, recent studies (see Reference (b) and (c) below) have shown that the direct and induced effects of lightning could damage an aircraft fabricated with all-composite material unless the electrostatic potentials were dissipated properly. Therefore, actual composite structured aircraft are expected to contain some form of protective metallic covering like conductive aluminum mesh imbedded in the epoxy laminate.

A differential sensor was included in Sensor Breadboard No. 1

Reference (b): Protection/Hardening of Aircraft Electronic Systems Against the Indirect Effects of Lightning; John C. Corbin, Jr., Atmospheric Electricity Hazards Group Air Force Flight Dynamics Laboratory Wright-Patterson AFB, Ohio 45433.

(c): Induced Effects of Lightning On An All Composite Aircraft; R. A. Perala, Electro Magnetic Applications, Inc., P. O. Box 8, Golden Colorado 80401 and K. Lee; Hughes Aircraft Corporation, Fullerton, R. Cook, Electro Magnetic Applications, Inc.

3.7 General Sensor Design Requirements

The function of a fault sensor is to detect a bus fault and cause the fault to be isolated prior to deactivation of the generating system. This is accomplished by sensing (1) overcurrent (+I, time or I^2t), (2) undervoltage (voltage, time), and (3) ground fault current (ΔI, time). The design limits of the sensors should include the time response characteristics of the Bus Power Controllers and the aircraft power management system. Accordingly, a total drop-out time of 20 milliseconds has been estimated for SOSTEL and the BPC's.

The fault current and associated voltage(s) are a function of the fault impedance. The maximum fault current was derived from a similar condition in Paragraph 4.6.9 of Reference (a), i.e., a fault impedance no less than 1 percent of the feeder impedance. In this study (FBFS), the feeder resistance was estimated to be as shown in Table 3.

The magnitude of the ground fault current is based on studies performed by Dalziel and Lagen (see Reference (d) below).

The voltage transient characteristics were obtained from Figure 2. Normal maximum bus currents are based on the Figure 1 power system configuration.

A summary of design and performance criteria for the FBFS study power distribution and sensor system in shown in Table 3.

Detail sensor design requirements are presented in the following section.

Reference (d): "Muscular Paralysis Caused by Electric Currents", Dalziel and Lagen, March 1941 issue of Electronics.

TABLE 3.

FBFS ELECTRIC POWER SYSTEM DESIGN & PERFORMANCE CRITERIA

CURRENT	
GENERATOR RATED CURRENT	333A
GENERATOR FAULT CURRENT LIMIT	500A
GENERATOR PARALLEL SYSTEM FAULT CURRENT LIMIT	1000A
GENERATOR FAULT CURRENT TIME LIMIT	7 Seconds
GENERATOR GROUND FAULT PROTECTION (AMP)	5.5 $\pm$ 0.5 ma
GENERATOR GROUND FAULT PROTECTION ACTUATION TIME	<20 ms
GENERATOR OVERLOAD	416A; (2) Min.
	500A; (7) Sec.
VOLTAGE	
NOMINAL (CENTRAL ELECTRONIC DIST. CENTER)	270 $\pm$ 5 Vdc
TRANSIENT VOLTAGE	Figure 2
GENERATOR UNDERVOLTAGE PROTECTION (Vdc)	240 $\pm$ 5 Vdc
GENERATOR UNDERVOLTAGE PROTECTION	$\geq$5 $\leq$7 Sec.
GENERATOR FEEDER	
CURRENT RATING	333A
LENGTH	15 Ft.
EQUIVALENT WIRE SIZE	#3/0
AMBIENT TEMPERATURE	100°C
RESISTANCE PER FEEDER DUAL (+) & (-)	$8.217 \times 10^{-4}\Omega$
AFT FEEDER	
CURRENT RATING	100A
LENGTH	25 Ft.
EQUIVALENT WIRE SIZE	#4
AMBIENT TEMPERATURE	20°C
RESISTANCE PER FEEDER EACH (+_ & (-)	$6.875 \times 10^{-3}\Omega$

SECTION IV
SENSOR DESIGN

4.1 Sensor Design Objectives

The proposed sensor system shown in Figure 4 requires the design of an overcurrent sensor, "+I", an undervoltage sensor, "+V", and a ground fault sensor, "ΔI". The following section lists the requirements derived for these sensors, based on the proposed power distribution system, followed by a description of the design of such sensors.

4.2 +I Overcurrent Sensor

The following are important characteristics or functions of an overcurrent sensor:

1) The type of current sensing element
2) Current range
3) Discrete number of fault thresholds that can be selected externally
4) A sensed current to reference comparator
5) A fault indication circuit
6) Electrical isolation between the bus and the monitoring system (in this case, SOSTEL)
7) I^2t function
8) Suitable electrical characteristics such as a low insertion loss, reasonable accuracy and frequency response
9) Small physical size

Figure 6 is a block diagram of a typical sensor configuration.

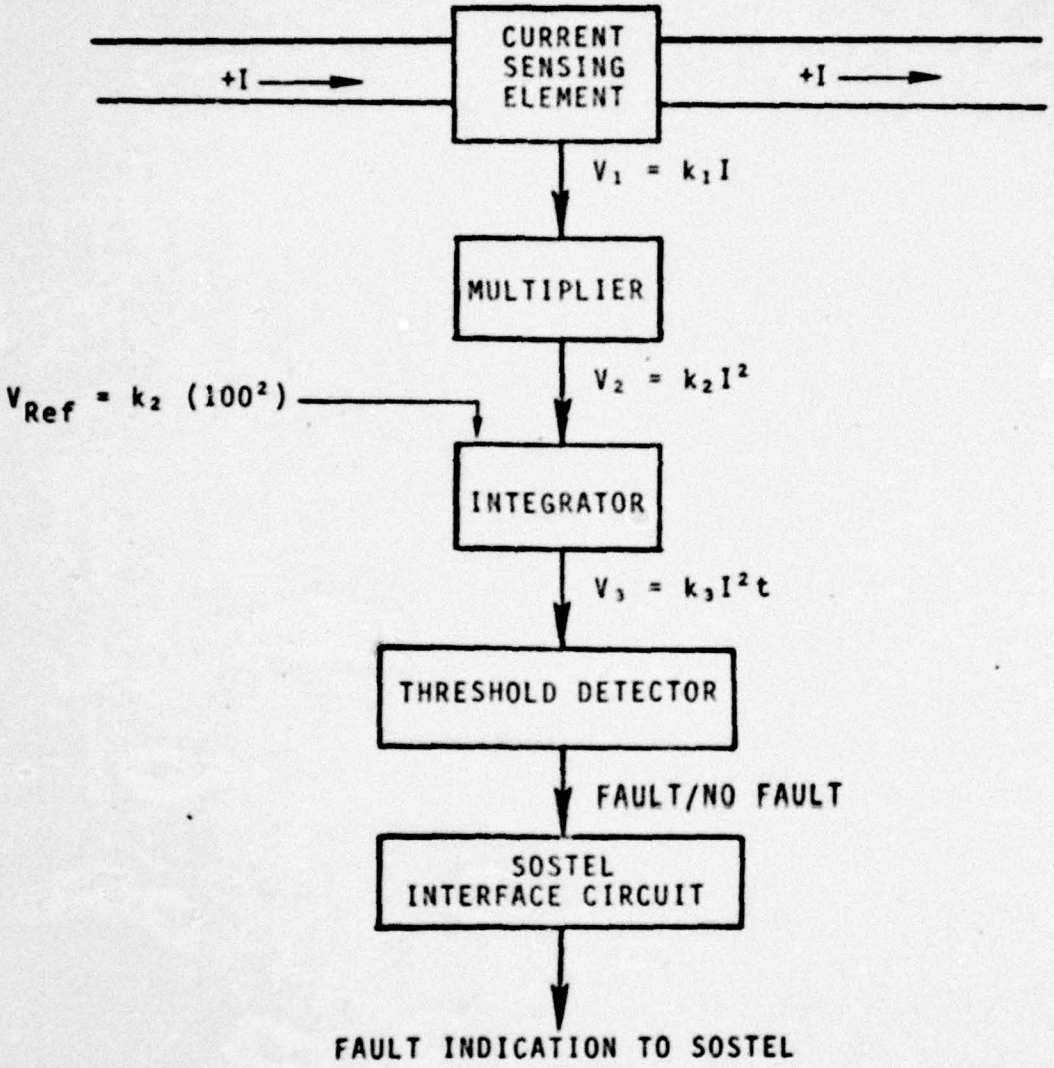

Figure 6. +I Overcurrent Sensor Block Diagram

4.2.1 +I Sensor Requirements

The following are the +I sensor requirements, based on the power distribution system shown in Figure 4, the performance criteria of Table 3 and the assumption that the sensor will be interrogated by SOSTEL:

Item	Bus Input	Sensor Output	SOSTEL Current
Normal Bus Current	$0 \leq I \leq 100A$	7.2 Vdc	10 mA
Bus Overcurrent	$>100A \leq 1000A$	4.2 Vdc	10 mA
Isolation	The resistance between the sensor outputs and the bus shall be a minimum of 1 megohm.		
Fault Output	All fault indications shall be sustained for a minimum of 30 milliseconds.		

4.2.2 +I Sensor Design Evaluation

Autonetics originally proposed sensing the magnetic fields produced by the bus current as the general approach for a fault current sensing element. A Hall Effect Device and dc transformers were the methods considered. Further investigations indicated that these methods could be used. However, the investigations also showed that modulating and demodulating the voltage sensed by a resistor in series with the bus offered more advantages than either of the two original methods. A brief description of the three types of current sensing methods considered follows.

Additional electronics is required to (1) compare the current sensed to some reference, (2) for developing the I^2t functions and (3) for providing the SOSTEL fault indication circuitry as shown in Figure 6. Since the development of the additional electronics is relatively straightforward and is common to all three sensing methods, it is not included in the following sensor comparison.

4.2.2.1 Dc Current Transformer as a Current Sensing Element

A block diagram of the dc current transformer circuit used as a current sensor is shown in Figure 7. The two cores are connected so that the ampere turns of one opposes the ampere turns of the other. When there is a dc current flowing in the sense winding, one core moves closer to saturation and the other moves further away. Full wave rectified current through R_L occurs as each core saturates on alternate cycles. The output voltage, V_{dc}, is thus directly proportional to the bias level set by I_{dc}.

Tests of the Figure 7 circuit indicated inaccuracies of the I_{in} to V_{dc} ratio of greater than 2% expected. Further development of this approach would probably achieve the desired accuracy. However, the estimated size (3 cubic inches) and the additional circuitry anticipated to eliminate the hysteresis affects for overcurrents of 1400A, plus the excellent results achieved with the modulator/demodulator approach (Paragraph 4.2.2.3) relegated this approach to a backup method.

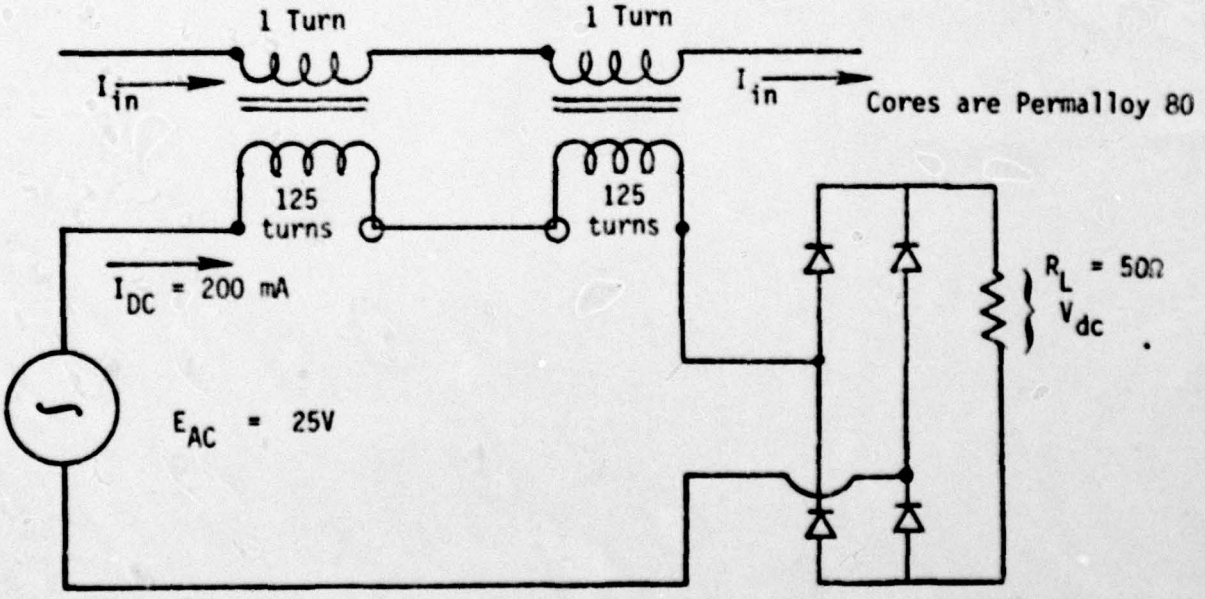

Figure 7. DC Current Transformer Block Diagram

4.2.2.2 Hall Effect Current Sensing Element

The Hall Effect arises from the fact that if a current carrying conductor is placed in a magnetic field, the moving charges will experience a net force mutually perpendicular to the direction of the current flow and the magnetic field. The resultant distortion in the local electric field gives rise to a voltage. In general, the relationship is:

$$V = \gamma IB$$

where V = Hall voltage
γ = a constant
I = bus current
B = magnetic field perpendicular to the Hall surface.

A Hall Effect Sensor proposed for the FBFS study had the following characteristics:

Current Range:	>1400A
Approximate Size:	1 in^3
Electric Isolation:	>1 megohm
Linearity:	$\pm$3%
Insertion Loss:	$\leq$0.05V
Sensitivity Drift:	$\leq$0.1%/ C
Offset:	$\leq$16 mV $\pm$ 40μV/$^{\circ}$C
Frequency Response:	dc to 400 Hz
Other:	Additional error ($\pm$16% in a typical design) may be caused by not centering the current cable in the sensor aperature.

Additional electronics is required to amplify the millivolt signals to a level suitable for detection.

The sensing inaccuracies as a function of changes in ambient temperature ruled out this sensing method as the desired approach.

4.2.2.3 Resistor as a Sensing Element

Measuring the voltage across a resistor in series with the bus was found to be the most desirable method of sensing the bus current. A block diagram of this method is shown in Figure 8. Based on independent research and development studies, manganin, a copper alloy that changes resistance less than ±1% from -55°C to 125°C and is 26 times as resistive as copper, is used as the sense resistor. However, any equivalent shunt element can be used. A modulator/demodulator circuit is used to provide the necessary electrical isolation and amplification. A typical sensing circuit using the Figure 8 approach has the following characteristics:

Current Range:	1400A
Output:	$V_o = 8.26\ (IR_s)^2 = K_6 I^2$
Accuracy:	2% of point or 2 mV, whichever is larger
Electrical Isolation:	>1 megohm
Temperature Range:	-55°C to 75°C
Approximate Size:	1 in³ (includes 0.05 X 0.8 X 1.4 inch manganin shunt)

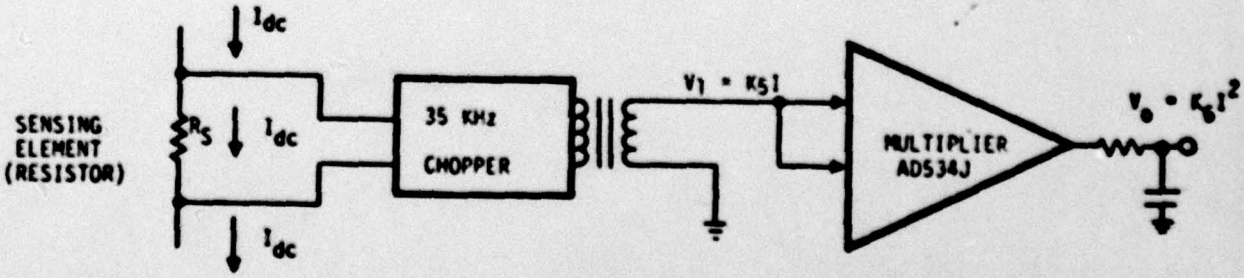

Figure (8). Block Diagram of Modulator/Demodulator Type of +I Current Sensor

4.2.2.4 Comparison of Current Sensing Methods.

Table 4 compares the three current sensing methods:

Item	DC Transformer	Hall Effect	Resistor + Mod/Demod
Assumed Current Range	0 - 1400A	0 - 1400A	0 - 1400A
Error	$\leq$ 2% (Estimated)	>3% (Calculated)	$\leq$ 3% (Test)
Output	$V_o = K_2 I$	$V_o = K_4 I$	$V_o = K_6 I$
Approximate Size	3 in^3	1 in^3	1 in^3
Electrical Isolation	>1 megohm	>1 megohm	>1 megohm
Insertion Loss	$\leq$0.05V	$\leq$0.05V	0.05V
Hysteresis Effects	Possibly	No	No

Table 4. Comparison of Current Sensing Methods

The modulator/demodulator method was selected as the most desirable approach, based on its higher accuracy, reasonable size, ease of fabrication and anticipated margin for further improvement.

4.3 +V Undervoltage Sensor

The following are the important requirements for an undervoltage sensor:

1) Undervoltage (235 V $\leq$ V $\leq$ 245 V) sensing capability
2) Electrical isolation (>1 megohm) between the bus and SOSTEL
3) Response time less than 7 milliseconds
4) Small physical size
5) All fault indications shall be sustained for a minimum of 30 milliseconds

A modulator/demodulator approach similar to the +I overcurrent design was selected as the configuration for the undervoltage sensor. Figure 9 is a block diagram of the sensor.

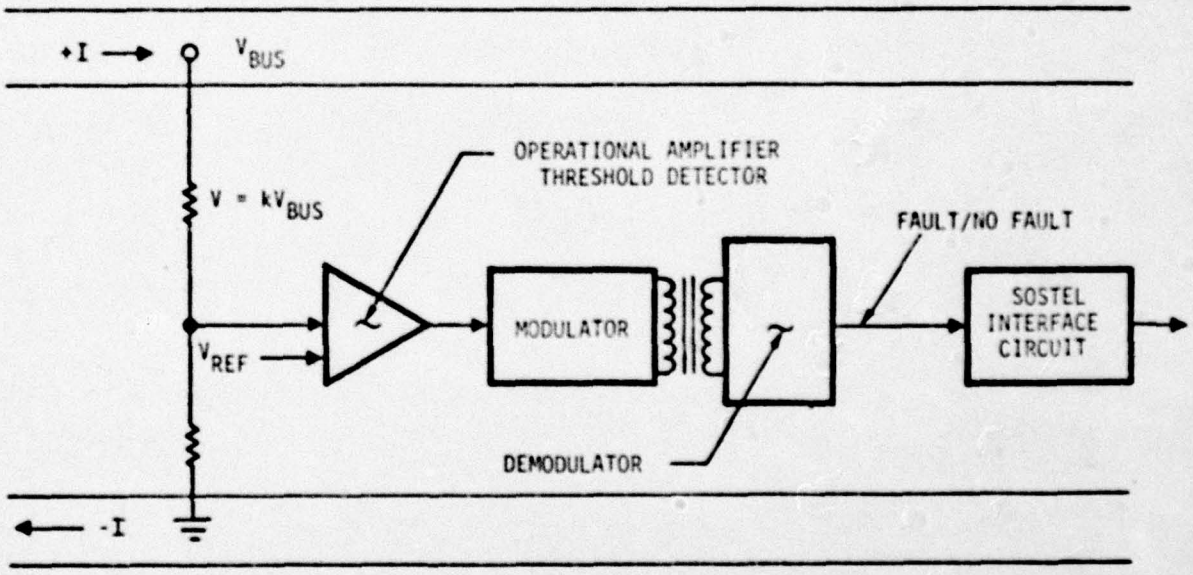

FIGURE (9). BLOCK DIAGRAM OF +V UNDERVOLTAGE SENSOR

The size of the sensor is approximately 2.2 in (1.5" X 2.2" X 0.7"); the response time was less than 2 milliseconds.

The Figure 9 mechanization achieves the electrical isolation required with minimum, readily available hardware. It has the additional advantage over the originally proposed configuration (Adc and μp) of "stand-alone" capability, i.e., it does not share a component part (Adc or μp) with another sensor. This sensing technique has been found to be satisfactory for all the deliverable breadboards.

4.4 ΔI Current Sensor

The primary requirement for this sensor is the ability to detect a difference of 6 milliamperes minimum between the nominal +100 ampere bus and the -100 ampere bus. The other standard sensor requirements still apply:

1) Electrical isolation (>1 megohm) between the bus and SOSTEL
2) Minimum physical size
3) All fault indications shall be sustained for a minimum of 30 milliseconds
4) Response time shall be less than 7 milliseconds.

A magnetic modulator approach was selected as the mechanization most likely to detect the less than 0.01% difference between the nominal source and return 100 ampere bus currents. Figure 10 is a simplified block diagram of this approach.

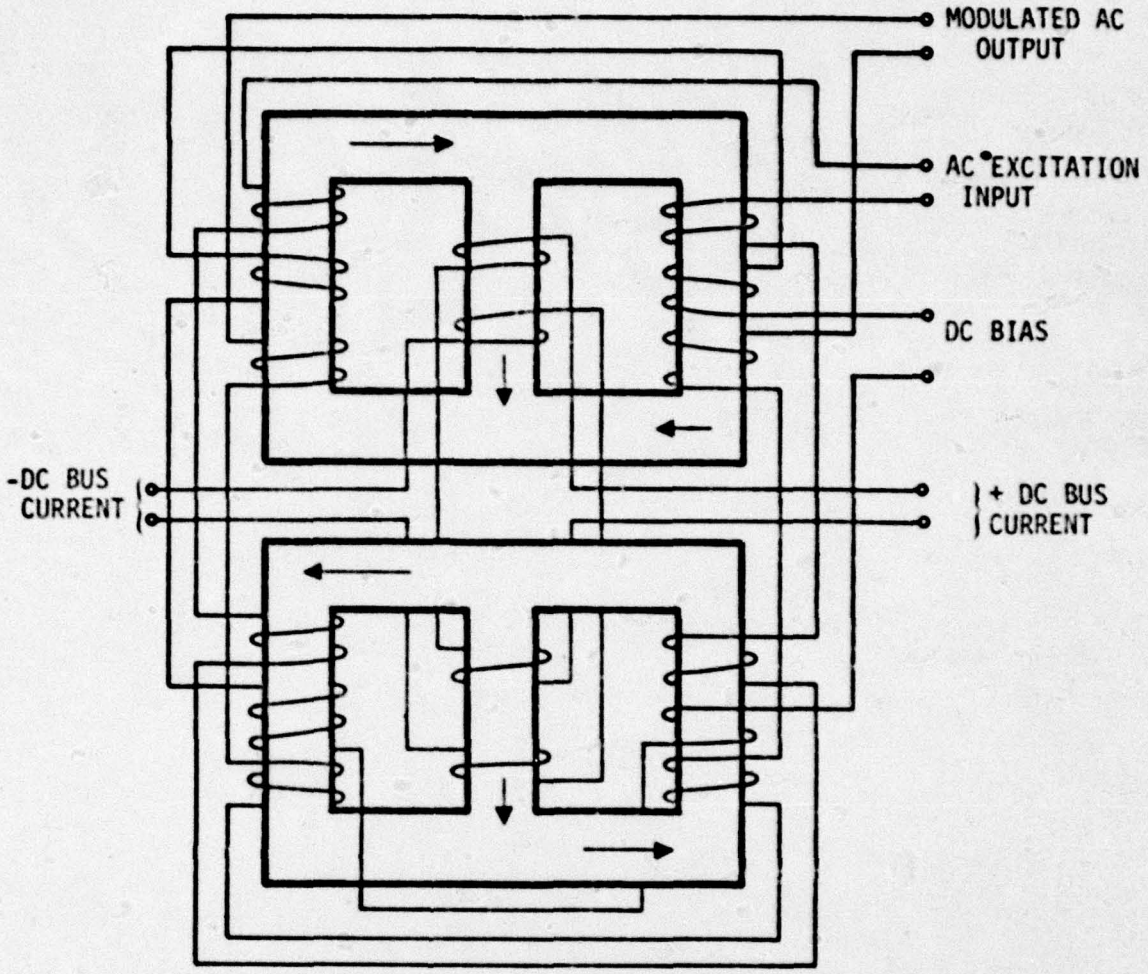

Figure (10). BLOCK DIAGRAM OF ΔI CURRENT SENSOR

The magnetic modulator is a dc to ac converter which provides a linear relationship between the difference in the dc bus currents and the modulated ac output. The magnetic modulator consists of two iron cores. On each core there are excitation, bias, signal (bus current) and output windings. Each of the related windings are connected in series. In this way, the current in both excitation windings, for example, will be equal. The same is true of the currents in the other windings. Both cores are of the same material and carefully matched to have the same magnetic characteristics. The bias winding provides constant flux in each core and the excitation current causes a flux variation proportional to excitation current. Therefore, both cores are operating about the same point in their respective magnetization curves and have flux variations which are equal

at all times; consequently, the dc output is zero. The + dc bus current windings are wound so that its ampere-turns oppose the ampere-turns of the bias winding in one core and aid the ampere-turns of the bias winding in the other core. The - dc bus current windings are wound opposite to the + dc windings. When bus current is imposed, the difference between the bus currents will move one core further into saturation and the other moves out of saturation. Because the modulator is now operating at different portions of the two curves, there will have a net flux linking with the output winding, producing an ac output. Negative feedback is used to control the gain throughout its operating range to produce a substantially linear output. A threshold detector within the ΔI Sensor produces a fault signal output when the difference in bus current exceeds 6 mA.

The characteristics of the ΔI Sensor are:

Current Range:	0 to 100 A
ΔI in Fault:	$\geq$ 6 mA
ΔI in Normal:	$\leq$ 5 mA
Electrical Isolation:	>1 megohm
Voltage Output:	0 to 0.4 Vdc, normal
	2.4 to 5 Vdc, fault
Size:	1.5" X 1.5" X 3"
Response Time:	$\leq$ 2 milliseconds

The sensor was particularly difficult to construct, due to the physical problems associated with winding the magnetic cores with the large guage wire required to sustain 100 amperes steady state. The sensor successfully detected 6 milliampere differences in the 100 ampere dc steady state currents. However, some difficulty was experienced in transient current cancellation. This difficulty was most likely a result of the winding problems mentioned above and could be eliminated by physical design refinements.

Since the aircraft may provide protection against ground faults, the detection of bus difference currents by the ΔI sensor provides questionable benefits because of its complexity and weight. Therefore, the ΔI sensor was included in Breadboard #1 only and was deleted from further study by program redirection in favor of additional effort in I^2t sensing techniques.

SECTION V
SENSOR BREADBOARDS

The subject contract required the fabrication, test and delivery of six sensor breadboards. The breadboards were configured to supply the sensors required by the results of the sensor system analysis. The general configurations of the breadboards are shown in Table 5.

Breadboard	Over Current	Under Voltage	Ground Fault	I^2t	Current Shunt	Power Supply
#1 (-1)	>100A	$\leq$235V	$\geq$6 mA	TBD	Internal	Internal $\pm$15vdc, +5Vdc regulators
#2 (-11)	>100A	$\leq$235V	No	4×10^4 at 100A	Internal	Internal $\pm$15 Vdc, +5 Vdc regulators
#3 (-21)	$>I=\frac{50\ mV}{R_S}$	$\leq$235V	No	4×10^4 at 100A	External	Internal $\pm$15Vdc, +5Vdc regulators
#4 (-41)	$>I=\frac{50\ mV}{R_S}$	$\leq$235V	No	4×10^4 at 100A	External	Internal $\pm$15Vdc regulators
#5 (-51)	$>I=\frac{50\ mV}{R_S}$	$\leq$235V	No	4×10^4 at 100A	External	Internal $\pm$15Vdc regulators
#6 (-51)	$>I=\frac{50\ mV}{R_S}$	$\leq$235V	No	4×10^4 at 100A	External	Internal $\pm$15Vdc regulators

Table 5. Sensor Breadboards

The salient features of the sensor breadboards are listed below:

(-1) FBFS Breadboard (Figure 11)

1) Provided laminated bus/connector to interface with flat bus ribbon cable.
2) Contained internal current shunt for 100A bus capability. However, shunt and shunt interconnecting wiring generated considerable heat.
3) Used TTL logic to generate SOSTEL signals.
4) Provided differential current sensor (ΔI); this sensor requires additional development because rapid changes in current may cause incorrect fault indication. This type of sensor later judged to be not necessary in FBFS.
5) Minimal I^2t capability; moderate I^2t capability can be achieved by increasing the capacitance of C_1 (Drawing No. 10160-507) and decreasing the resistance of R_1.

(-11) FBFS Breadboard (Figure 12)

1) Implemented improved I^2t function.
2) Eliminated ΔI current sensing.
3) Reduced internal heating by providing means for direct connection to current shunt resistor.

(-21) FBFS Breadboard (Figure 13)

1) Replaced internal shunt resistors with provisions to connect to a selectable external shunt. This satisfies the pin programmable requirement in that it allows operation at various maximum current levels. Selectable shunts within the sensor would have required a considerable increase in volume and elaborate mechanical design.
2) New 4 X 4 X 2 inch package and an eight pin interface connector.

(-41) FBFS Breadboard (Figure 14)

1) Switched to VMOS transistors for the SOSTEL output devices. This was desirable because of the relatively high V_{ce} saturation voltage of the TTL devices.

2) Used CMOS for the "one-shot" and logic gates to minimize power consumption and eliminate the need for a +5 volt regulator.

3) Eliminated the diode from the integrator and changed the RC timing so that the LF356 would slew from positive to negative saturation. This increases the accuracy and the adjustment range.

(-51) FBFS Breadboard (Figure 15)

1) Changed integrator RC to a 4700 PF 1% glass capacitor and a 511K 1% resistor to provide more stable timing. Some remaining integrator offset drift indicates that further stabilization of the integrator may be desirable. A chopper stabilized amplifier is a possible alternative.

2) Design of an overcurrent sensor using a length of copper wire in place of an internal manganin or external current shunt did not prove to be feasible at this time. The major problem area was the difficulty in maintaining the ratio of resistance of the sensor current path to that of the resistance of the various parallel copper bus shunts to the accuracy required over the entire operational temperature range.

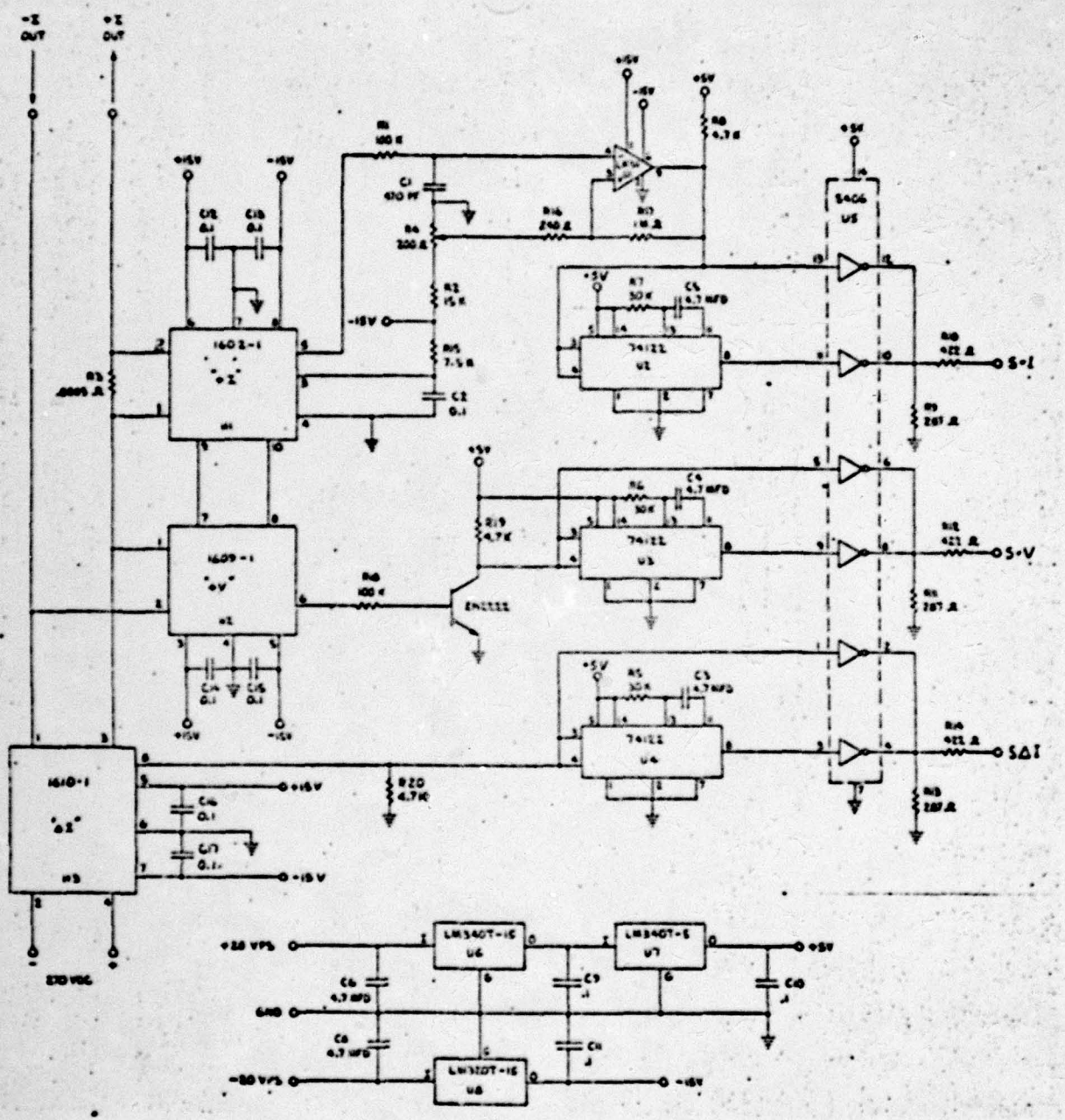

FIGURE (11). -1 ASSEMBLY SCHEMATIC DIAGRAM

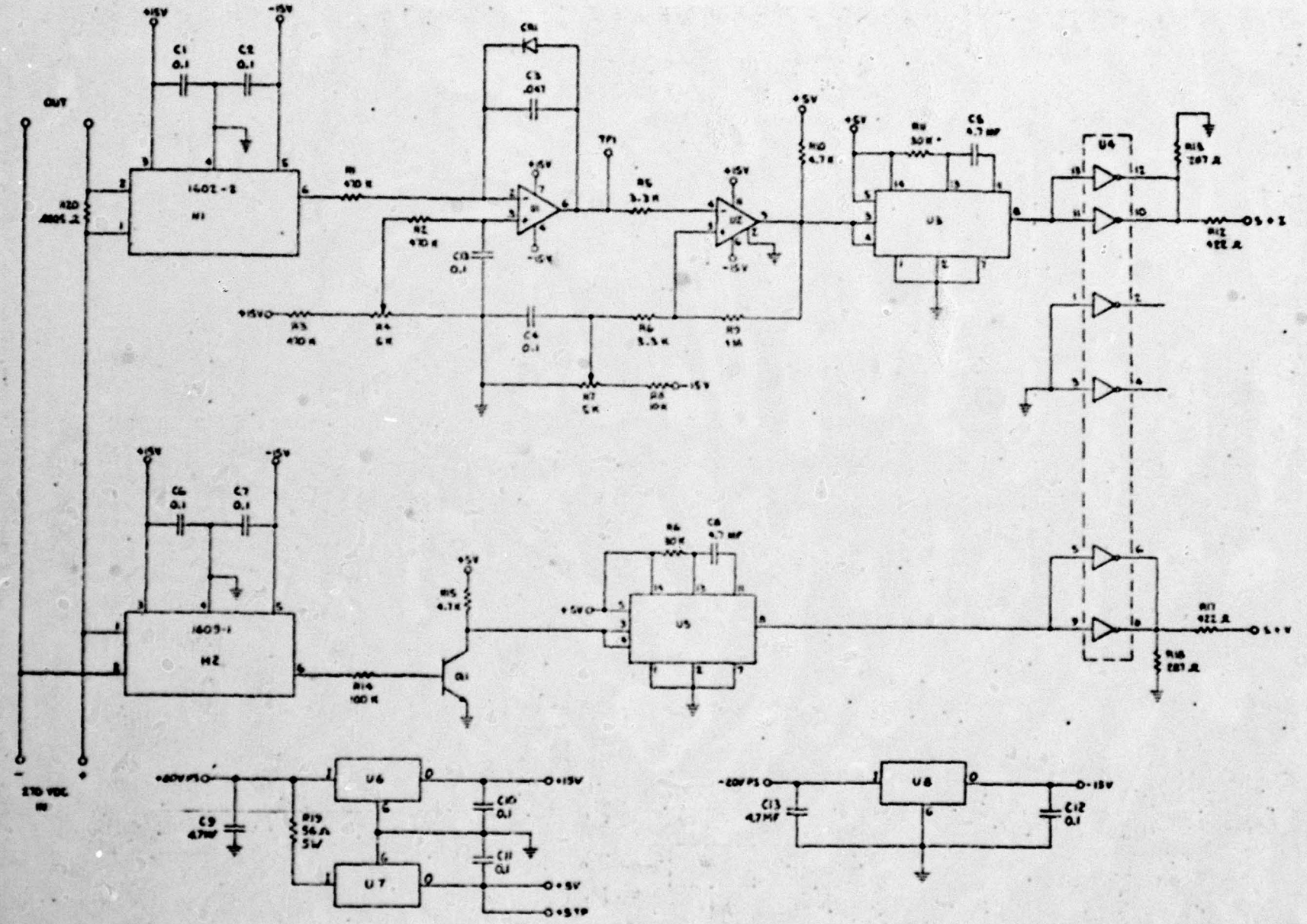

FIGURE (12). -11 ASSEMBLY SCHEMATIC DIAGRAM

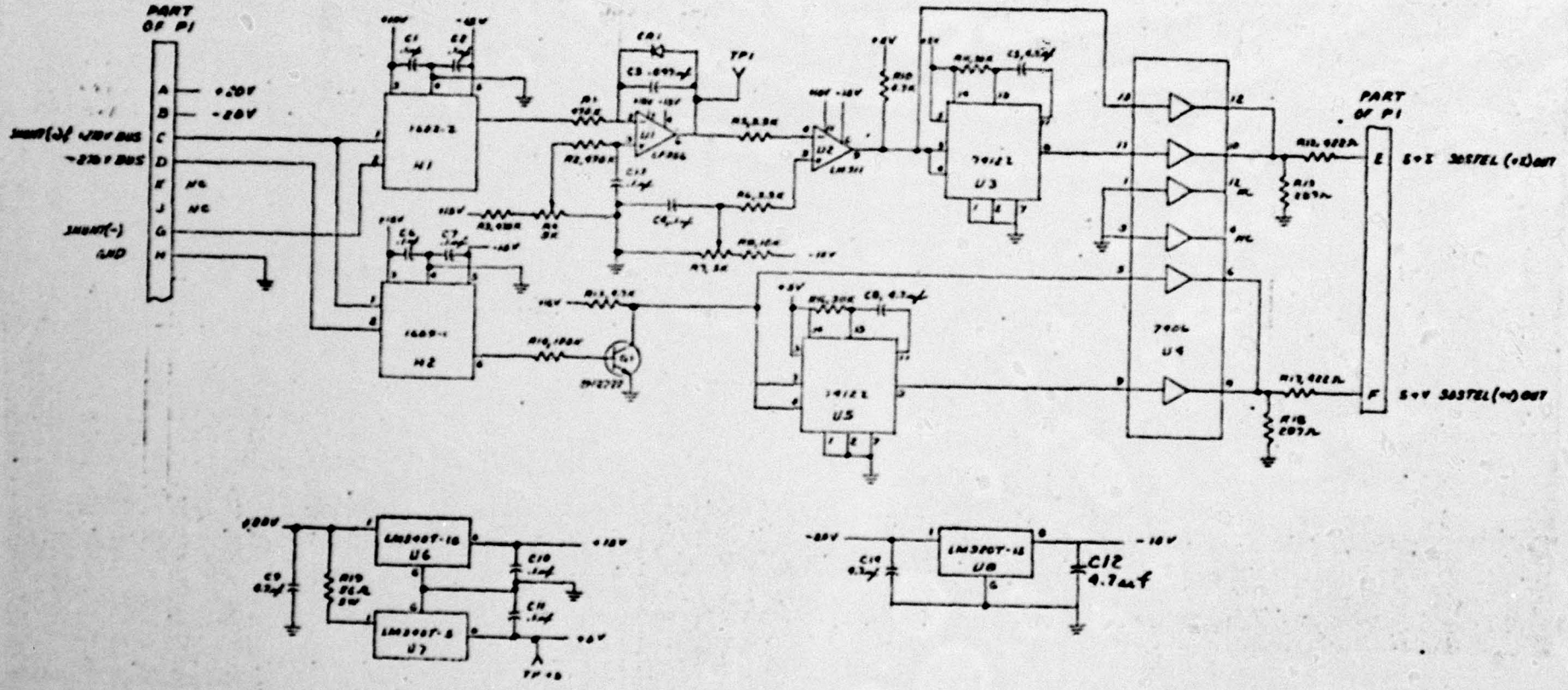

FIGURE (13). -21 ASSEMBLY SCHEMATIC DIAGRAM

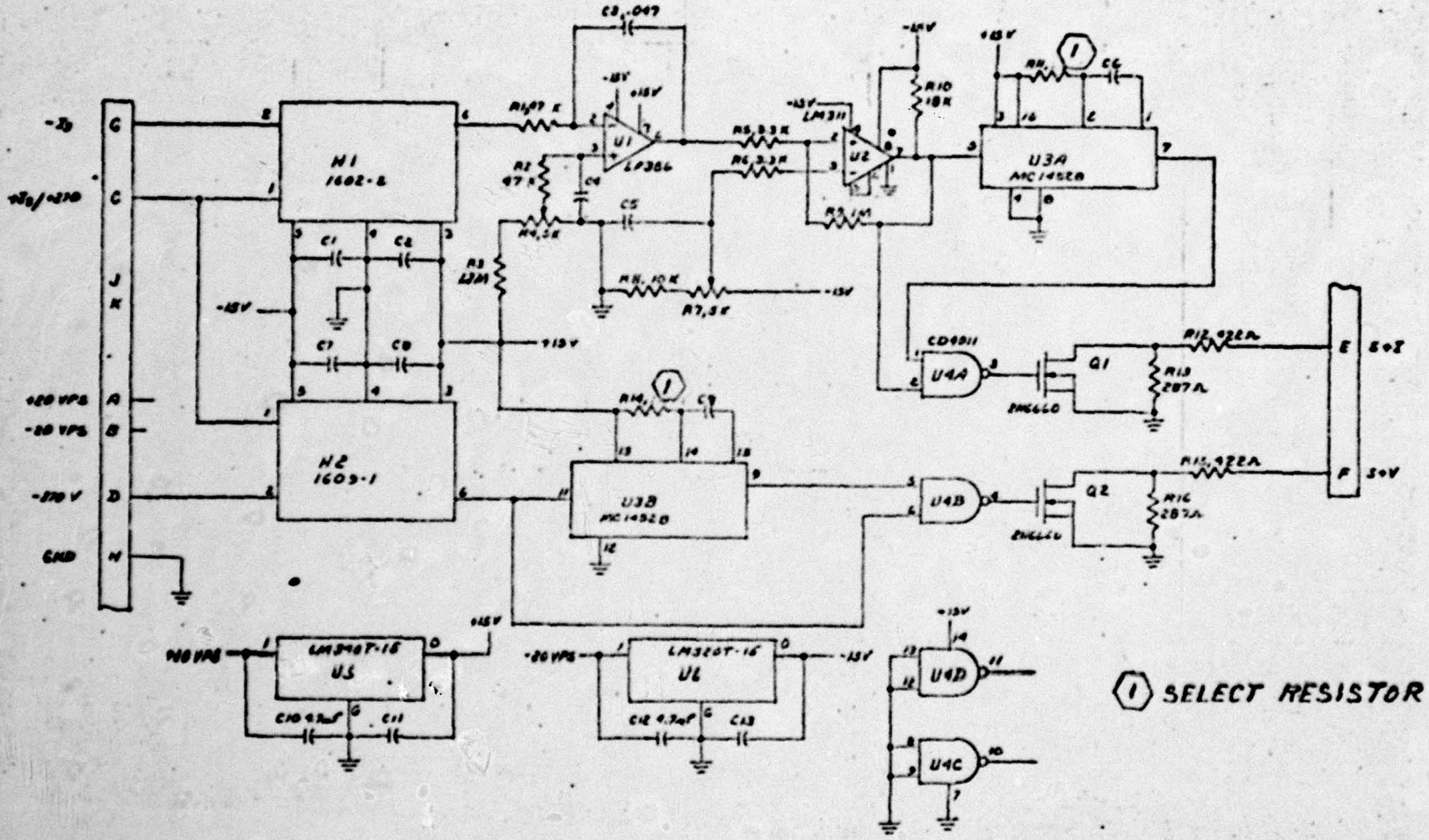

FIGURE (14). -41 ASSEMBLY SCHEMATIC DIAGRAM

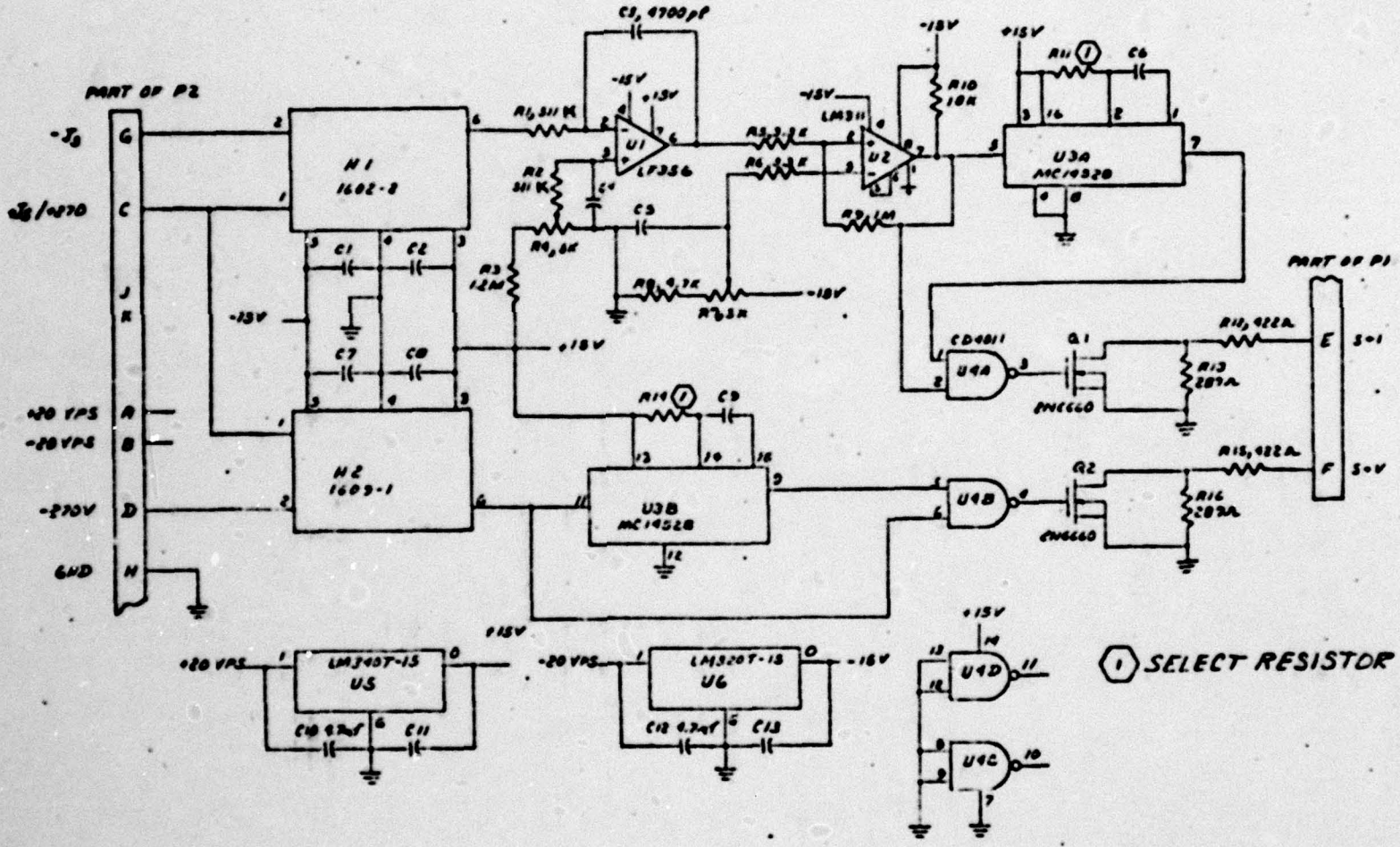

FIGURE (15). -51 ASSEMBLY SCHEMATIC DIAGRAM

SECTION VI
CONCLUSIONS

1) The sensor system depicted in Figure 4 together with the power system performance criteria of Table I meet the stated objectives of the Flat Bus Fault Sensor Study.

2) The +I, +V and ΔI sensor fulfill the requirements for fault sensors that sense line-to-line and line-to-structure faults.

3) The breadboards described in Paragraph 5.0 can be used to demonstrate the feasibility of the sensing concept developed.

The study also indicated that all three types of sensors (+I, +V and ΔI) are necessary for a complete fault current sensor system. Each sensor type provides a unique function.

Based on independent investigations (References b and c), an ungrounded aircraft power distribution system fabricated with composite material will require some form of structure ground system. This re-introduces the possibility of ground faults and therefore, the need for a ΔI sensor, either as part of the generator or as part of the distribution system.

It is concluded that further refinements of the +I and +V sensors can be achieved by electrically isolating the sensors at the SOSTEL/Sensor interface. This would allow using the +270 volt bus as a power source for the sensors and eliminate the need for a power supply in each sensor.

It is also concluded that using an external current shunt is the most practical method of providing a programmable +I sensor due to the appreciable power dissipation of an internal current shunt.

SECTION VII
RECOMMENDATIONS

The initial intent in the Flat Bus Fault Sensor Study was to use the sensors in a two-wire ungrounded electrical power system in a composite type aircraft structure; however, independent investigations have indicated that a purely composite structure may be susceptible to lightning, EMP and EMI to a detrimental degree. This suggests the need for some type of protective grounding system in the composite structure. The definition of such a grounding system is recommended.

It is recommended that the development of the +I and +V sensors proceed from breadboard to prototype designs. Design improvements can be achieved in the areas of packaging and power dissipation.

In Figure 4, approximately 50% of the +I sensors operate in conjunction with an adjacent Bus Power Controller. Combining these two elements (+I sensor and BPC) into one functional unit, i.e. a power controller with I^2t trip capability would probably be a very desirable simplication in terms of hardware and functional capability. The power controller would trip with an overcurrent in the event that SOSTEL failed to open the adjacent power controller. Thus, a fail-safe capability would be added to the sensor-power controller set without requiring additional hardware.

A hybrid type of power controller developed by the Autonetics Division of Rockwell International is recommended for this type of controller. The hybrid controller consists essentially of a solid state switch in parallel with an electro-mechanical contactor. The solid state section is used to connect and disconnect power to the load and the contactor is used to conduct the steady current. This method insures arcless switching and consequently long contact life. A current sensor and a microprocessor is used for the I^2t and switch functions.

Flat cable technology should be investigated to establish methods of interfacing the sensors and current shunts to the flat busses.

In summary, the FBFS concept offers significant fault detection capability to the AAES System and should be developed further.

APPENDIX A

GLOSSARY OF TERMS

A	Ampere
AAES	Advanced Aircraft Electrical System
AC	Alternating Current
ADC	Analog-to-Digital Converter
BPC	Bus Power Controller
BTC	Bus Tie Controller
C	Capacitance
DC	Direct Current
E	Electromotive Force
EMI	Electro Magnetic Interference
EMP	Electro Magnetic Pulse
FBFS	Flat Bus Fault Sensor
Ft.	Foot
GPC	Generator Power Controller
In.	Inch
+I	Bus Current From The Generator
-I	Bus Current To The Generator
+I #1	Overcurrent Sensor #1
ΔI #1	Differential Current Sensor #1
KHz	Kilohertz
LPC	Load Power Controller
mA	Milliampere
Min.	Minute
μp	Microprocessor
NADC	Naval Air Development Center
pA	Picoampere
PC	Power Controller
Sec	Second
SOSTEL	Solid State Electric Logic
Sq.	Square
V	Volt
+V #1	Undervoltage Sensor #1
V/STOL	Vertical Short Take Off and Landing